

Hydrobiologia

Spatial patterns of morphological variability of the eelpout *Austrolycus depressiceps* (Teleostei: Zoarcidae) across western Patagonia

--Manuscript Draft--

Manuscript Number:	
Full Title:	Spatial patterns of morphological variability of the eelpout <i>Austrolycus depressiceps</i> (Teleostei: Zoarcidae) across western Patagonia
Article Type:	Primary research paper
Keywords:	latitudinal gradient; geometric morphometrics; morph; freshwater input; phenotype
Corresponding Author:	Mauricio F. Landaeta, Dr. Universidad de Valparaiso Viña del Mar, Valpararaiso CHILE
Corresponding Author Secondary Information:	
Corresponding Author's Institution:	Universidad de Valparaiso
Corresponding Author's Secondary Institution:	
First Author:	Fernanda S. Orrego, BSc
First Author Secondary Information:	
Order of Authors:	Fernanda S. Orrego, BSc Mathias Hüne, MSc. Hugo A. Benítez, PhD Mauricio F. Landaeta, Dr.
Order of Authors Secondary Information:	
Funding Information:	Instituto Antártico Chileno (RT_08-18) Dr. Mauricio F. Landaeta
Abstract:	Phenotypic variation in organisms depends on the genotype and the environmental constraints of the habitat that they exploit. Therefore, for marine species inhabiting contrasting aquatic conditions, it is expected to find covariation between the morphospace and hydrography. We studied the phenotypic variability of the head and cephalic sensorial canals of the eelpout <i>Austrolycus depressiceps</i> (4.5-22.5 cm TL) across its latitudinal distribution in western Patagonia (45°S-55°S). Geometric morphometric analyses show that morphospace varied from individuals with larger snout and an extended suborbital canal to individuals with shorter snouts and frontally compressed suborbital canal. The ontogenetic allometry was low, with a decrease of the relative size of the eye. Individuals from the northernmost locations showed robust heads while those from the south had slender head, with a pointed snout. Seawater salinity covaried with shape of the head; in brackish waters, eelpouts had slender head and snout, smaller eyes, and horizontally oriented mouth, while in saltier waters individuals had robust head, shorter snout, bigger eyes and oblique mouth. The morphospace of marine fish with shallow distribution across Patagonia are influenced by salinity (i.e., phenotypic modulation), and may be sensitive to the ice melting of Northern and Southern Icefields caused by global warming.
Suggested Reviewers:	Alberto T. Correia, PhD Researcher, Universidade Fernando Pessoa acorreia@ufp.edu.pt Dr. Correia has vast experience in the utilization of geometric morphometrics in describing fish phenotypic variability Brian Sidlauskas, PhD Researcher, Oregon Agricultural College: Oregon State University

brian.sidlauskas@oregonstate.edu
Dr. Sidlauskas has vast experience in fish morphology and ecological and evolutionary variation

Dominique Ponton, PhD
Professor, Universite de Toliara
dominique.ponton@ird.fr
Dr. Ponton has wide experience in the use of geometric morphometrics in marine fish morphological variation

1 Submitted to Hydrobiologia as Primary Research Paper

2

3

4

5

6 **Spatial patterns of morphological variability of the eelpout *Austrolycus depressiceps***

7 **(Teleostei: Zoarcidae) across western Patagonia**

8

9 Fernanda S. Orrego¹, Mathias Hüne², Hugo A. Benítez³, Mauricio F. Landaeta^{1,4,5*}

10 ¹Laboratorio de Ictioplancton (LABITI), Instituto de Biología, Facultad de Ciencias, Universidad de
11 Valparaíso, Valparaíso, Chile

12 ²Centro de Investigación para la Conservación de los Ecosistemas Australes (ICEA), Punta Arenas,
13 Chile

14 ³Laboratorio de Ecología y Morfometría Evolutiva, Centro de Investigación de Estudios Avanzados
15 del Maule, Universidad Católica del Maule, Talca, Chile

16 ⁴Centro de Observación Marino para Estudios de Riesgos del Ambiente Costero (COSTA-R),
17 Universidad de Valparaíso, Viña del Mar, Chile

18 ⁵Millennium Nucleus for Ecology and Conservation of Temperate Mesophotic Reef Ecosystems
19 (NUTME)

20

21 *Corresponding author. Email: mauricio.landaeta@uv.cl

22 Mauricio F. Landaeta ORCID-ID: 0000-0002-5199-5103; Mathias Hüne ORCID-ID: 0000-0003-
23 0089-7623; Hugo Benítez ORCID-ID: 0000-0001-7553-9893

24

25 Short title: Phenotypic variation in zoarcid *Austrolycus depressiceps*

26

27 Abstract

28 Phenotypic variation in organisms depends on the genotype and the environmental
29 constraints of the habitat that they exploit. Therefore, for marine species inhabiting contrasting
30 aquatic conditions, it is expected to find covariation between the morphospace and hydrography. We
31 studied the phenotypic variability of the head and cephalic sensorial canals of the eelpout *Austrolycus*
32 *depressiceps* (4.5-22.5 cm TL) across its latitudinal distribution in western Patagonia (45°S-55°S).
33 Geometric morphometric analyses show that morphospace varied from individuals with larger snout
34 and an extended suborbital canal to individuals with shorter snouts and frontally compressed
35 suborbital canal. The ontogenetic allometry was low, represented by a decrease of the relative size of
36 the eye, and a depression of the posterior margin of the head. Individuals from the northernmost
37 locations showed robust heads while those from the southern tip of South America had a slender head,
38 with a pointed snout. Seawater salinity covaried with shape of the head; in brackish waters, eelpouts
39 had a slender head and snout, smaller eyes, and horizontally-oriented mouth, while in saltier, oceanic-
40 influenced waters, individuals had robust head, shorter snout, bigger eyes and oblique mouth opening.
41 Two of the canals of the cephalic lateralis pores and the head shape showed modularity in its
42 development. This study shows that the morphospace of marine fish with shallow distribution across
43 Patagonia are influenced by salinity (i.e., phenotypic modulation), and may be sensitive to the ice
44 melting of Northern and Southern Icefields caused by global warming.

45 Keywords: latitudinal gradient; geometric morphometrics; morph; freshwater input; phenotype

46

47 **Funding**

48 This work was partially funded by the Chilean Antarctic Institute project INACH RT_08-18 grant to
49 MFL.

50 **Conflict of interest**

51 The authors have no financial or proprietary interests in any material discussed in this article

52 **Availability of data and material**

53 Data will be available upon reasonable request.

54 **Code availability**

55 Not applicable.

56 **Author's contribution**

57 **MH** collected the fish, measured it and took the photographs, **FSO** digitized the landmarks and
58 performed data analysis, **HAB** performed modularity data analysis, **MFL** wrote the first version of
59 the manuscript; the whole team wrote the final version of the manuscript.

60

61 **Introduction**

62 Phenotypic plasticity is one of the mechanisms for explaining why populations or species
63 may differ phenotypically, in which a single genotype expresses different phenotypes in response to
64 different environmental signals (Sultan 2011). Two types of phenotypic plasticity can be defined,
65 developmental conversion, and phenotypic modulation. The first one results in discrete morphs in
66 response to an environmental cue. In contrast, phenotypic modulations result in continuous variation
67 of a particular trait in response to an environmental stimulus (Stearns 1989). Thus, at large
68 distributional scales, trait variation patterns can provide insights into micro- and macroevolutionary
69 patterns, indicating selective agents responsible for major trends for phenotypic evolution and local
70 adaptation (Riesch et al. 2018). Latitudinal variation in body size (the Bergmann's rule) has been
71 linked to fitness, with larger body size in colder environments, i.e., towards higher latitudes (Ouyang
72 et al. 2018).

73 The extensive Chilean Patagonia (41°S-56°S) is characterized by high degree of
74 geomorphological and hydrographic complexity, with innumerable channels and fjords, which have
75 been molded by ice expansion and contraction during the Quaternary glacial period (Hulton et al.
76 2002; Sudgen et al. 2002). These generate highly heterogeneous marine habitats that are heavily
77 influenced by freshwater discharges from precipitation and glacier melting (Dávila et al. 2002), which
78 give this region high environmental variability. Two large temperate icefields, the Northern
79 Patagonian icefield and Southern Patagonian icefield, represent 83% of the total ice loss in the
80 southern Andes, and are responsible for a total of 3.3 mm of sea-level rise between 1961 and 2006
81 (Bravo et al. 2021). Additionally, and because of the latitudinal extension of Patagonia, important sea
82 surface temperature gradients also occur, varying from 4 to 18 °C (Bruno et al. 2018, Molina-Valdivia
83 et al. 2021). This environmental variability as well as coastal geometry may impact on the body shape
84 variability in terrestrial (i.e., rodents, Valladares-Gómez et al. 2020) and marine species with shallow
85 vertical distribution, such as some endemic eelpouts.

86 Eelpouts of the family Zoarcidae are a group of 47 genera and about 240 valid species of
87 marine perciform fishes. Twenty-one of these fish species have been recorded in the Chilean

88 Patagonia (Hüne 2019). They are the most diverse family of the suborder Zoarcoidei and exhibit a
89 greater degree of character plasticity than the other families (Anderson and Fedorov 2004). It is
90 considered as monophyletic and has four subfamilies, Lycozoarcinae, Zoarcinae, Gymnelinae and
91 Lycodinae. These fish can be found over a wide range of depths: most zoarcids are deep-water benthic
92 species, but some southern hemisphere species inhabit intertidal areas (Gosztonyi 1977). Zoarcids
93 have elongated, eel-like bodies and as a group show modest diversification in form (Lannoo and
94 Eastman 2006).

95 Vision in zoarcids is reduced, and specimens rely on olfaction and taste to detect prey (Fanta
96 et al. 2001, Lannoo and Eastman 2006), based on the peripheral lateral-line system. This system is
97 composed of canal neuromasts (CNs) occurring in canals on fishes' heads and trunks. CNs function
98 as pressure gradient detectors, i.e., they respond to pressure differences between neighbouring canal
99 pores (Mogdans 2019), and are distributed into supra and infraorbital, the otic and postotic and the
100 mandibular and preopercular canals (Anderson 1994, Mogdans 2019). It is unknown whether
101 morphological integration occurs between sensory canals and head shape during ontogeny of
102 Zoarcidae. In this sense, morphological integration describes the correlation among traits and occurs
103 when changes in one trait are accompanied by changes in other traits that are affected by common
104 mechanisms such as developmental pathways, genetic linkages and functional activities (Adams
105 2016).

106 The genus *Austrolycus* belongs to Lycodinae, and it is composed of two species, *A.*
107 *depressiceps* Regan, 1913 and *A. laticinctus* (Berg, 1895). The genus is characterized by the absence
108 of pyloric caeca, 6-7 suborbital pores, and a single postorbital pore above the gill slit (Anderson
109 1994). The latter species have more caudal vertebrae (80-89) than the first (72-79) (Anderson and
110 Gostonyi 1991). *Austrolycus depressiceps* is a medium-size zoarcid (4-41 cm length), living among
111 macroalgae, below rocks and stones, in the subantarctic waters of South America, from the intertidal
112 down to 12 m depth (Moreno and Jara 1984, Hüne et al. 2021). They are sedentary and sluggish
113 (Vanella and Calvo 2005). Females deposit egg masses below stones in the intertidal zones. Eggs are
114 nearly spherical and large (9.2-9-8 mm), as well as the size of the recently hatched larvae (22 to 25
115 mm, Matallanas et al. 1990). Juveniles feed on small crustaceans (isopods, amphipods, polychaetes),
116 while adults are ichthyophagous, predated on *Harpagifer bispinis* and *Patagonotothen cornucola*
117 (Matallanas 1988; Lloris and Rucabado 1991). This species has a wide geographic range throughout
118 the west Patagonia, from Aysen (47°S) to Diego Ramírez Island (56°30'S), and off Argentina and
119 Malvinas/Falkland Islands (Pequeño 1986, Reyes and Hüne 2012).

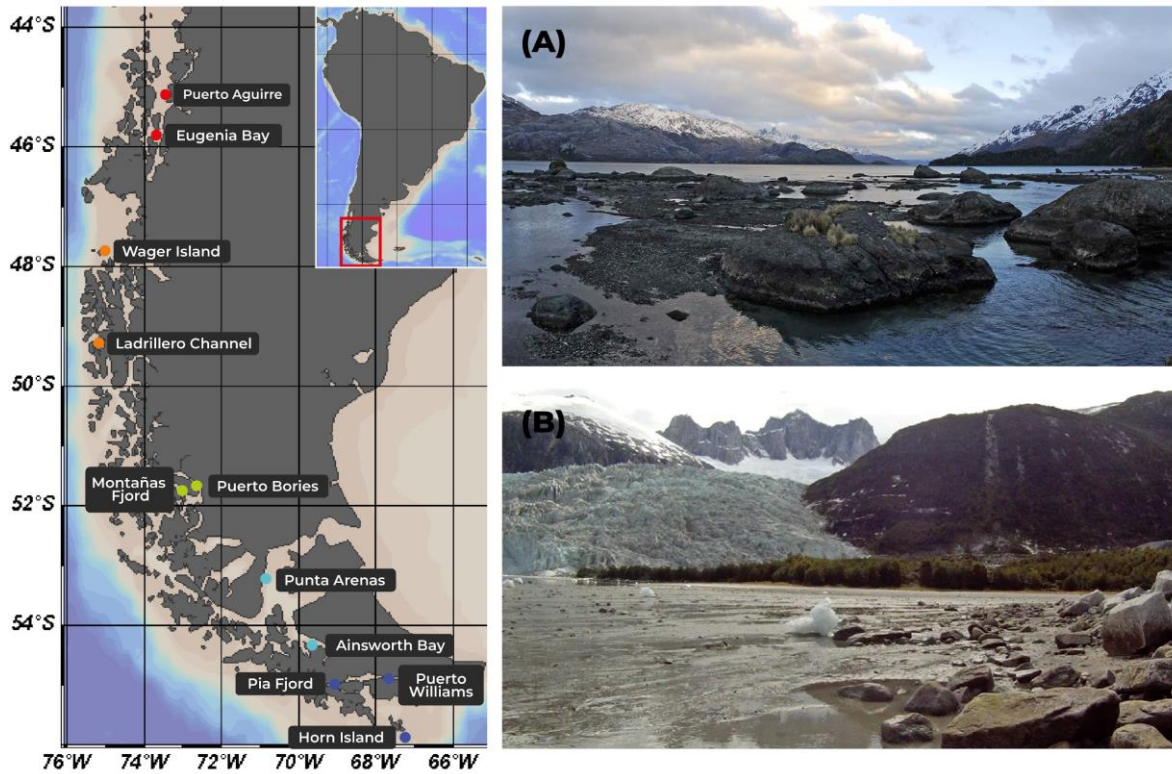
120 Based on the large spatial distribution of *A. depressiceps* along the western Patagonia, we
121 expect to find latitudinal gradients of the shape of the head and the relative location of the sensory
122 canals, expressed as well as in changes in body mass condition. Our goal is to describe the variability
123 of the morphospace of the head and some cephalic lateralis canals located in the head, at ontogenetic
124 and large spatial scales (hundreds of kilometres), and the integration/modulation of the head and its
125 canals throughout the life history of the eelpout.

126

127 **Materials and Methods**

128 Field collection and measurement

129 Adult fish ($n = 126$) were collected between 2007 and 2020 at 11 intertidal locations across
130 the western coast of Patagonia, covering most of the spatial distribution of the species (Fig. 1). Sea
131 temperature and salinity were obtained at each sampling site with multiparameter sondes (YSI 556
132 and YSI 6920 v2) (Table 1). All fish were captured by hand and with hand nets during diurnal low
133 tide periods (Fig. 1 A-B). Specimens were preserved in 96% ethanol for subsequent examination. All
134 specimens were measured for total length (TL, cm) and total weight (g) and photographed from a
135 lateral view using a digital SLR camera (Nikon D850) fitted with a microlens (AF-S Nikkor 60 mm).
136 The species is sexually monomorphic, so we did not distinguish between males and females in the
137 following analyses.



139

140 Figure 1. Sampling locations of *Austrolycus depressiceps* along the western coast of Patagonia.
 141 Photos of some intertidal locations: (A) Montañas Fjord, and (B) Pia Fjord.

142

143 Data analysis

144 Length-weight relationship was fitted by a power model: $Y = aX^b$, where Y = weight, and X
 145 = total length. The Fulton index of condition, $K = 1000 \times (M / L^3)$, where M is the mass and L is the
 146 length, was estimated separately for each specimen. Additionally, the Relative condition (K_n) was
 147 computed as the observed individual mass (M_i) divided by the predicted mass (M_i^* , where $M_i^* = aL_i^b$,
 148 and a and b are the parameters of the length-weight relationship).

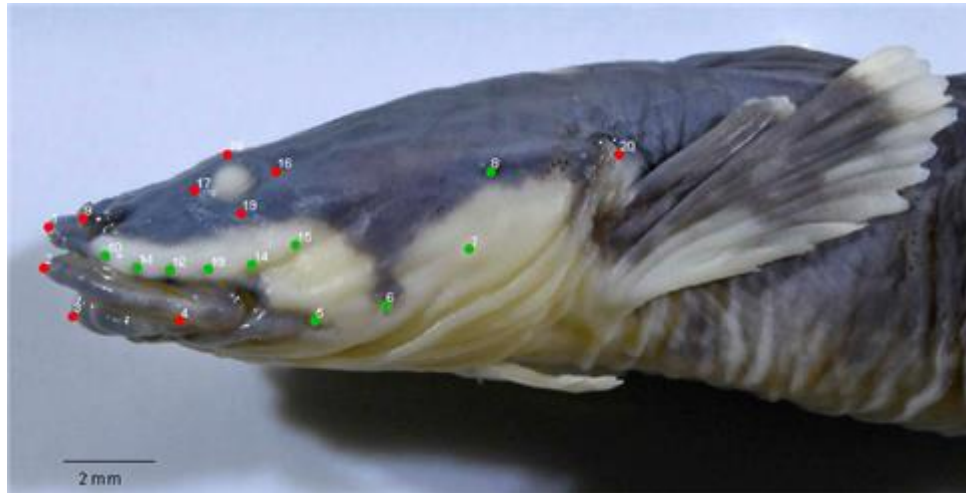
149 Locations were grouped into zones in order to represent a latitudinal gradient (Fig. 1, Table
 150 1): North of Taitao Peninsula (NTP, Puerto Aguirre, Eugenia Bay), Central Channels (CCh, Wager
 151 Island, Ladrillero Channel), Central Fjords (CF, Montañas Fjord, Puerto Bories), Magellan Strait
 152 (MS, Punta Arenas, Ainsworth Bay), and Beagle Channel (BC, Pia Fjord, Puerto Williams, Horn
 153 Island). Comparison of K and K_n were made among zones using one-way ANOVA and Tukey's post
 154 hoc tests, because data showed normal distribution (Shapiro-Wilk's test, $W = 0.98$, $P > 0.085$).

155 Table 1. Locations and sampling dates where the eelpout *Austrolycus depressiceps* were collected
 156 across the Chilean Patagonia, as well as the *in situ* hydrographic conditions.

Zones	Location	Sampling date	Latitude	Longitude	Temperature (°C)	Salinity (PSU)
NTP	Puerto Aguirre	14-01-2017	-45.159	-73.531	12.61-12.63	27.33-27.32
NTP	Eugenia Bay	30-10-2007	-45.948	-73.569	11.51	26.1
CCh	Wager island	02-02-2016	-47.753	-74.999	11.83-11.94	30.15-30.22
CCh	Ladrillero Channel	20-03-2010	-49.178	-75.397	11.03-11.64	31.20-31.60
CF	Montañas Fjord	04-04-2009	-51.778	-73.330	7.2	16.45
CF	Puerto Borjes	10-03-2008	-51.690	-72.542	8.23-9.93	14.11-14.51
MS	Punta Arenas	03-03-2009	-53.307	-70.934	7.80-7.87	30.19-30.62
MS	Ainsworth Bay	10-01-2020	-54.406	-69.621	7.13	28.42
BC	Pia Fjord	18-12-2011	-54.793	-69.600	6.55	14.1
BC	Puerto Williams	10-12-2008	-54.931	-67.577	7.75-7.86	28.62-28.70
BC	Horn Island	15-02-2017	-55.959	-67.230	9.16	33.51

157

158 For the geometric morphometric analyses, a database with images of 126 specimens was
 159 created using the program TPSUtil 1.60. A 20-landmark configuration (Fig. 2) was then digitized
 160 onto each photograph and a replica of each image using the software TPSDig 2.17. This landmark
 161 configuration aimed to reflect the shape of the mandible apparatus (premaxilla, maxilla, dentary, LM
 162 1-4), eye (LM 16-19), head (LM 1 and 20), as well as the location of the nostril (LM 9) and the
 163 arrangement of some cephalic lateralis canals, such as the suborbital canal (LM 10-15), the
 164 preopercular portion of the preoperculo-mandibular canal (LM 5-7) and the postorbital pore 4 (LM
 165 8). Shape information was extracted from the landmark coordinates with a Generalized Procrustes
 166 analysis (GPA) using MorphoJ 1.06d (Klingenberg 2011), in which coordinates were scaled,
 167 translated and rotated onto a common coordinate system to extract the shape variation from each
 168 individual and remove size and rotation influences (Rohlf and Slice 1990). Residuals from the
 169 consensus configuration were modeled with the thin-plate spline (Bookstein 1992). To assess the
 170 measurement error, a Procrustes analysis of variance (Procrustes ANOVA) was carried out using
 171 MorphoJ software.



172

173 Figure 2. Eelpout *Austrolycus depressiceps* from west Patagonia, showing the distribution of
 174 landmarks on the head (red dots) and on selected sensory canals (green dots). 1. Mesethmoid; 2.
 175 Anterior margin of the premaxilla; 3. Anterior margin of the dentary; 4. Posterior margin of the
 176 dentary; 5-7. preoperculo-mandibular pores; 8. postorbital pore; 9. nostril; 10-15. Suborbital pores;
 177 16. Anterior margin of the eye; 17. Posterior margin of the eye; 18. Lower margin of the eye; 19.
 178 Upper margin of the eye; 20. Posteriormost margin of the operculum.

179

180 A Principal component analysis (PCA) was performed using the shape coordinates to identify
 181 the main axes of shape variation, as well as specific changes in the head and pores. For the
 182 visualization, a warping transformation grid was used following Klingenberg (2013). To quantify the
 183 ontogenetic effect in the shape change (ontogenetic allometry), a multiple regression between
 184 Procrustes coordinates and log centroid size (a proxy of size) was done (Loy et al. 1998). Residuals
 185 of the ontogenetic allometry relationship were used for comparisons of the morphospace among
 186 zones, by a Canonical Variate Analysis (CVA) and Bonferroni-corrected multiple comparisons using
 187 the Procrustes distances and permutation tests.

188 Additionally, a two-block, partial least squares (PLS) between condition indices (K and Kn),
 189 sea temperature and salinity (Block 1) and Procrustes coordinates (Block 2), were run, for testing for
 190 covariation between shape, body mass condition of the eelpout and sea water conditions across
 191 western Patagonia. PLS is a method for extracting the eigenvectors and eigenvalues from two blocks
 192 of covarying data. Also, for the estimation of the strength association between blocks, the Escoufier's
 193 RV coefficient and a permutation test were estimated (Goswami and Polly 2010, Klingenberg 2009).

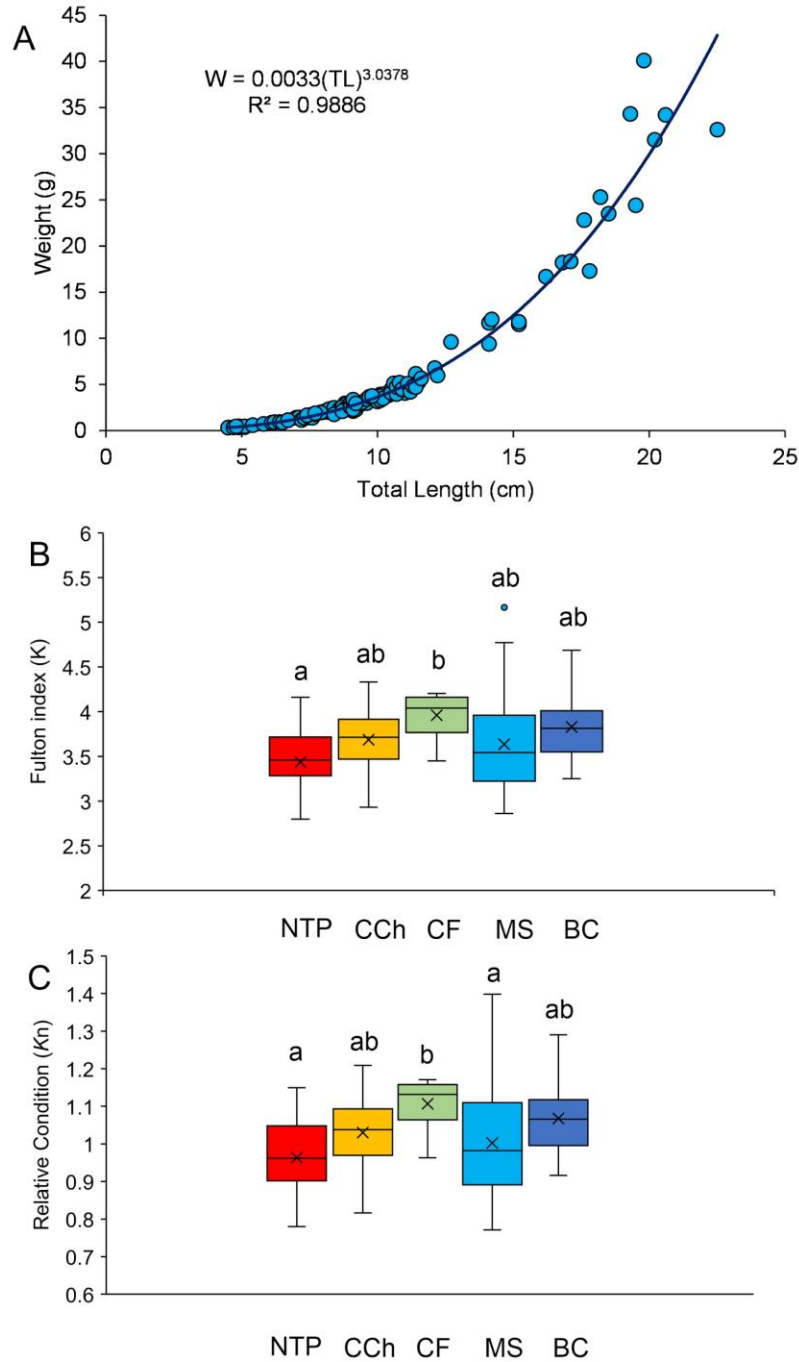
194 Finally, two modularity hypotheses were tested between the head (red landmarks in Fig. 2)
195 and sensory canals (green landmarks in Fig. 2), a *functional hypothesis* (H1) and a *structural*
196 *hypothesis* (H2). H1 assumes that the sensory canals and the anterior morphology (neurocranium, oral
197 jaw apparatus) have different, but complementary functions (i.e., prey detection and capture,
198 respectively), especially under low-light conditions (Mogdens 2019), such as the turbid, coastal
199 waters of west Patagonia (>4 NTU, Castillo-Hidalgo et al. 2018). By contrast, H2 is a hypothesis of
200 developmental modularity derived from the observation that zoarcid have different rates of
201 ossification during larval development (Voskoboinikova and Laius 2003), and the opercular region
202 (where the preoperculo-mandibular canal is located) increases its relative size during early
203 development (Marcinkevicius and Gosztanyi 2013). Integration between modules will be measured
204 using the covariance ratio test (CR), which can be defined as the ratio of the overall covariation
205 between modules relative to the overall covariation within modules (Adams 2016). All statistical
206 analyses were performed using MorphoJ 1.06d and *geomorph 4.0* R package (Adams & Otárola-
207 Castillo 2013), and the new package *gmShiny* using the new modules of *geomorph* (Baken et al.
208 2021).

209

210 **Results**

211 Size distribution, length-weight relationships and condition

212 Specimens collected varied between 4.5 and 22.5 cm TL (mean \pm SD, 9.94 ± 3.69 cm) and
213 from 0.316 to 40.100 g (5.43 ± 7.75 g). The length-weight relationship showed a positive allometry
214 ($b = 3.03$), and a larger dispersion in bigger specimens (between 13-23 cm TL, Fig. 3A). The analysis
215 of K indicated that those specimens collected north of Taitao Peninsula (NTP) were significantly in
216 poor condition than those from Central Fjords (CF; one-way ANOVA, $F = 7.24$, $P < 0.0001$; Tukey
217 test, $P = 0.002$) (Fig. 3B). Similarly, K_n varied significantly (one-way ANOVA, $F = 7.55$, $P = 0.001$)
218 among zones, with specimens from CF being in better condition than those from NTP and MS (Fig.
219 3C).



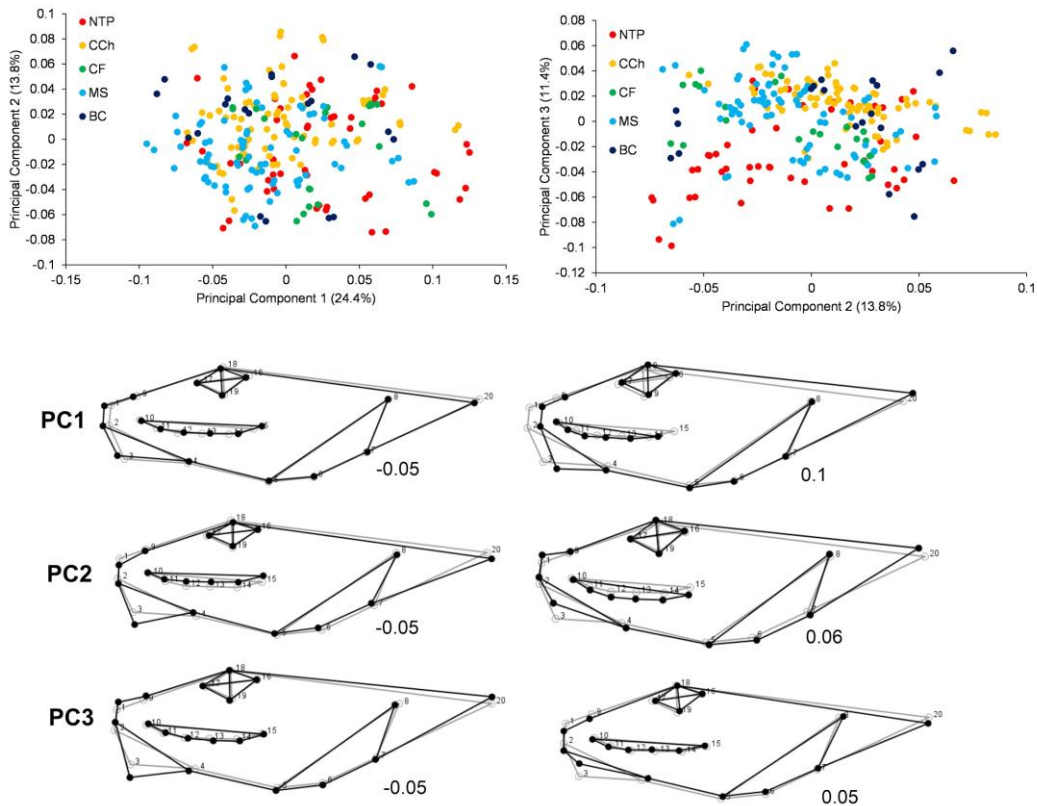
220

221 Figure 3. A. Length-weight relationship of the eelpout *Austrolycus depressiceps* from western
 222 Patagonia; B. Comparison of the Fulton's index of condition (K); C. Comparison of the Relative
 223 Condition (K_n) among sites, North of Taitao Peninsula (NTP), Central Channels (CCh), Central
 224 Fjords (CF), Magellan Strait (MS) and Beagle Channel (BC). Different letters indicate significant
 225 differences ($P < 0.05$).

226

227 Shape changes and ontogenetic allometry

228 Procrustes ANOVA estimated that the measurement error (i.e., landmark digitalization)
 229 explained 3.09% of the total variance ($F = 31.29$, $P < 0.0001$). The variability of the morphospace of
 230 adult *A. depressiceps* was explored using PCA. The PCA was explained by 36 principal components,
 231 from which the first 14 explained 90% of the total variance.



232

233 Figure 4. Shape changes of the head and sensory canals of the eelpout *Austrolucys depressiceps* from
 234 west Patagonia. NTP: North of Taitao Peninsula, CCh: Central Channels, CF: Central Fjords, MS:
 235 Magellan Strait, BC: Beagle Channel. Grey wireframes represent the consensus morph (0,0), while
 236 the black wireframes represent the final morph. The number under each wireframe represents the
 237 scale along each principal component.

238 PC1 (24.49%) was explained mainly by the horizontal displacement of the suborbital pores
 239 4, 5 and 6 (LM 14-16), and the horizontal displacement of the anterior margin of the dentary (LM 3),
 240 mesethmoid (LM 1) and premaxilla (LM 2) (Table 2). These relative displacements indicate the
 241 presence of specimens with larger snout and an extended suborbital canal (i.e., suborbital pores 5 and
 242 6 located behind the posteriormost margin of the eye) vs. specimens with shorter snouts and frontally
 243 compressed suborbital canal (i.e., suborbital pores 5 and 6 posteriorly extended to the level of the

244 middle of the eye), respectively (PC1 Fig. 4). The PC2 explained 13.8% of the shape variance and
 245 represented the vertical displacement of the anterior margin of the dentary (LM 3), and the
 246 mesethmoid (LM 1) and oblique displacement of the operculum (LM 20). This means a shape
 247 variability from individuals with pointed snout, closed mouth and smaller head to specimens with
 248 rounded snout, open mouth and larger head (PC2 Fig. 4, Table 2). Finally, the PC3 explained 11.4%
 249 of the variance, and represented the opposite of the PC2, specimens with pointed snout, open mouth
 250 and shorter head *vs.* specimens with rounded snout, closed mouth and larger head (Fig. 4, Table 2).
 251 Because the position of the dentary (closed *vs.* opened mouth) depends on the *post-mortem* conditions
 252 rather than the morphological features of the individual, both PCs represent specimens with pointed
 253 snout and shorter head and those with rounded snout and larger head.

254

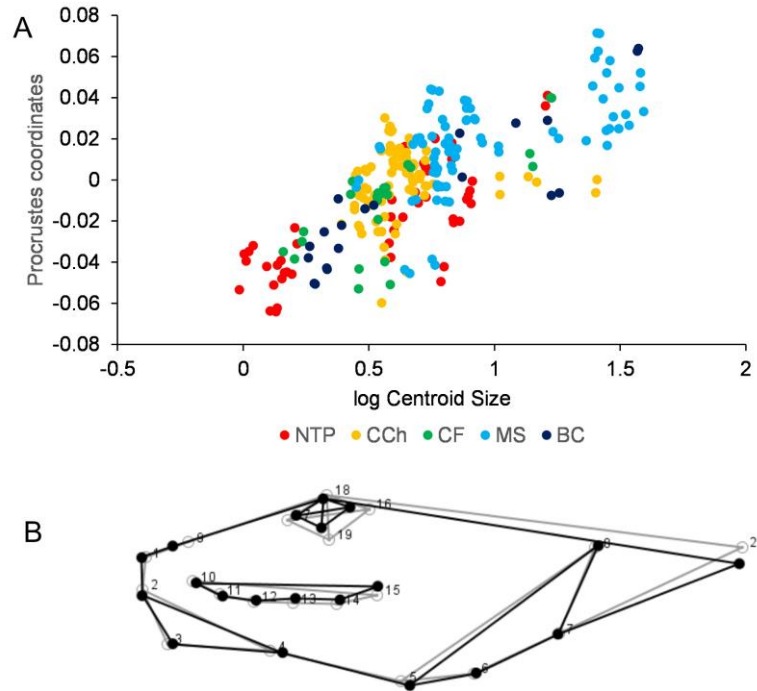
255 Table 2. Landmark configuration in the head of the eelpoul *Austrolycus depressiceps*. Bold numbers
 256 indicate those landmarks showing the most noticeable changes at each Principal Component (PC).

Morphological trait	LM	PC1	PC2	PC3
Mesethmoid	x1	0.282	0.026	-0.076
	y1	0.016	0.281	-0.342
Anterior margin of the premaxilla	x2	0.276	-0.026	-0.011
	y2	0.029	0.228	-0.343
Anterior margin of the dentary	x3	0.302	-0.077	0.020
	y3	-0.149	0.554	0.572
Posterior margin of the dentary	x4	-0.033	0.148	0.282
	y4	-0.085	-0.173	0.093
Preoperculo-mandibular pore 5	x5	0.002	0.114	0.063
	y5	-0.057	-0.074	0.115
Preoperculo-mandibular pore 6	x6	-0.019	0.154	0.006
	y6	-0.027	-0.099	0.100
Preoperculo-mandibular pore 7	x7	-0.053	0.118	0.035
	y7	-0.025	-0.108	0.072
Postorbital pore 4	x8	0.026	-0.024	0.180
	y8	-0.005	0.092	0.046
Nostril	x9	0.189	0.042	-0.099
	y9	0.025	0.065	-0.201
Suborbital pore 1	x10	-0.058	0.044	-0.085
	y10	0.020	-0.042	-0.055
Suborbital pore 2	x11	-0.173	0.033	-0.098
	y11	0.025	-0.110	-0.031
Suborbital pore 3	x12	-0.270	0.001	-0.143

	y12	-0.014	-0.203	0.021
Suborbital pore 4	x13	-0.351	-0.029	-0.168
	y13	-0.023	-0.229	0.087
Suborbital pore 5	x14	-0.405	-0.050	-0.132
	y14	-0.032	-0.243	0.064
Suborbital pore 6	x15	-0.355	-0.056	-0.075
	y15	-0.115	-0.274	0.025
Anterior margin of the eye	x16	0.141	-0.027	0.026
	y16	0.086	0.032	0.010
Posterior margin of the eye	x17	0.078	-0.086	0.143
	y17	0.037	-0.005	-0.014
Inferior margin of the eye	x18	0.108	-0.081	0.057
	y18	0.080	0.096	-0.012
Superior margin of the eye	x19	0.094	-0.014	0.103
	y19	0.041	-0.076	0.073
Posteriormost margin of the operculum	x20	0.220	-0.211	-0.027
	y20	0.173	0.289	-0.280

257

258 The multiple regression between shape (Procrustes) coordinates and log centroid size was
259 significant ($P < 0.001$) and 4.71% of the total variance was explained by the ontogenetic allometry
260 (Fig. 5A). The main changes through ontogeny were the decrease of the relative size of the eye, and
261 a deepening of the upper margin of the operculum, which may be representing a depression of the
262 posterior margin of the head (Fig. 5B). A slight elevation of the suborbital pores 5 and 6 (LM 14 and
263 15, respectively) and a frontal displacement of the nostril (LM 9) were also observed.



264

265 Figure 5A. Ontogenetic allometry of the eelpout *Austrolycus depressiceps* (Zoarcidae) from west
 266 Patagonia. NTP: North of Taitao Peninsula, CCh: Central Channels, CF: Central Fjords, MS:
 267 Magellan Strait, BC: Beagle Channel. B. Shape changes during ontogeny. Grey wireframes represent
 268 the starting morph, while the black wireframes represent the final morph.

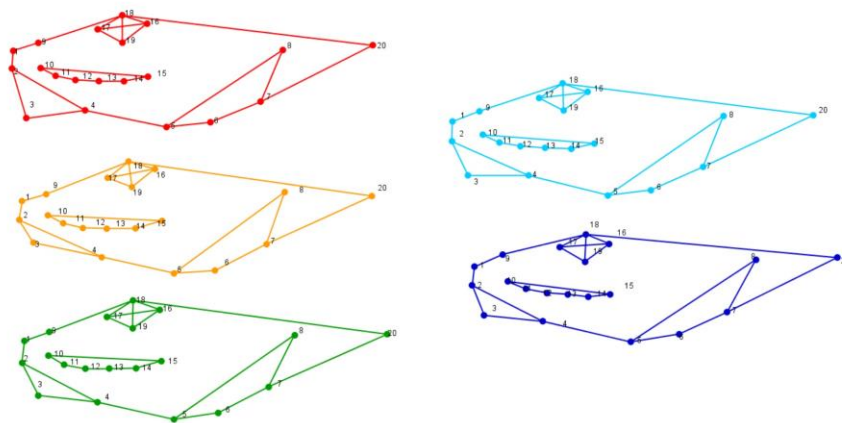
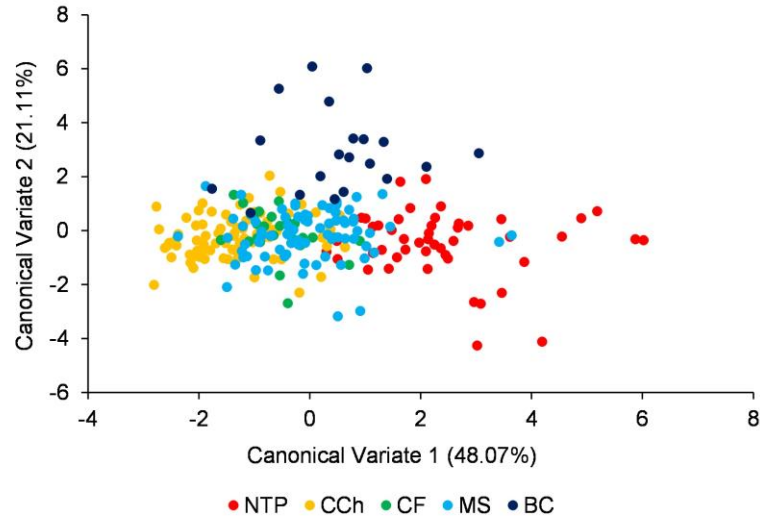
269

270 Spatial variability of *A. depressiceps* shape

271 The comparison of the shape among zones was explained by four Canonical Variates, in
 272 which the first two CVA showed noticeable differences in the shape of the eelpout among zones (Fig.
 273 6). A permutation test based on Procrustes distances detected significant differences in the morph
 274 among zones (Bonferroni corrected P values, $P < 0.001$). The differences were more pronounced
 275 between the northern (NTP) and southern (BC) extremes of the spatial distribution: while in NTP (red
 276 in Fig. 6) the shape of the head was robust, expressed by a dorsal location of the eye and open mouth
 277 (vertical displacement of the point of the dentary), specimens from BC showed a slender head, with
 278 a more pointed snout (blue in Fig. 6). Additionally, specimens from channels and fjords (CCh and
 279 CF) showed a concave snout, caused by a deeper position of the nostril (LM9) (Fig. 6).

280

281



282

283 Figure 6. Canonical Variate Analysis (CVA) comparing the morph of the eelpout *Austrolycus*
 284 *depressiceps* among zones of west Patagonia. NTP: North of Taitao Peninsula, CCh: Central
 285 Channels, CF: Central Fjords, MS: Magellan Strait, BC: Beagle Channel. The consensus morph of
 286 each zone is shown by different colours.

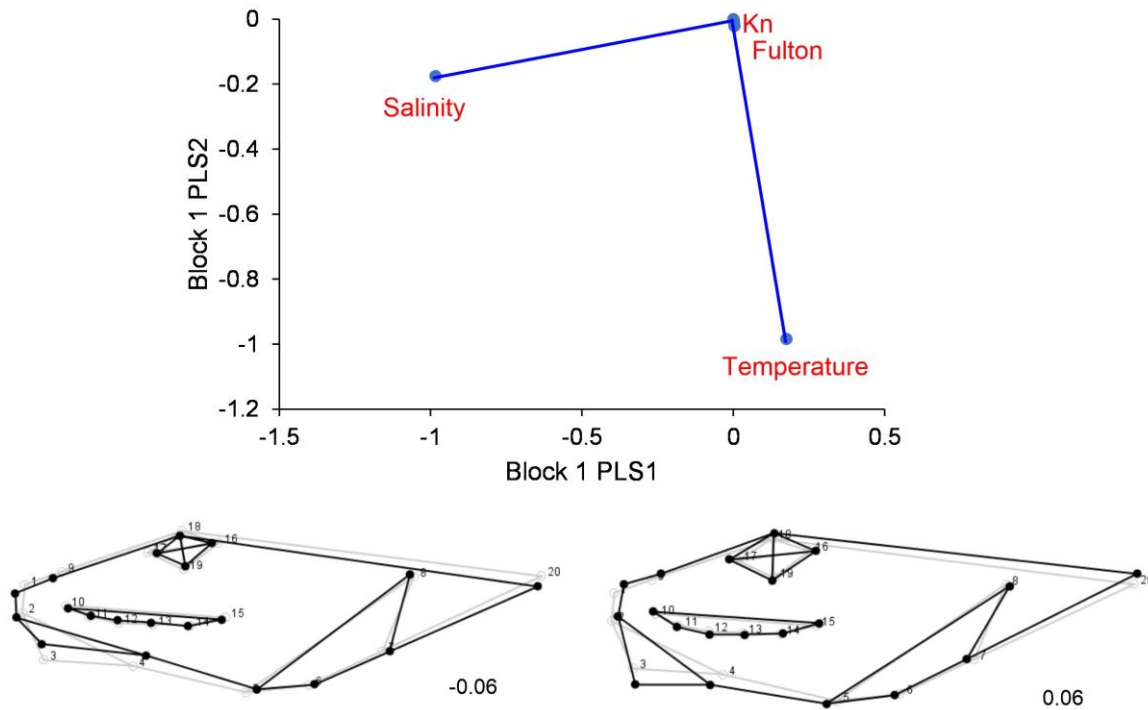
287

288 Shape, body mass and sea water conditions

289 The PLS showed covariance between Block 1 and Block 2, explained by four PLS. The PLS1
 290 explained 76.4% of the covariance, with significant correlation between PLS1 of block 1
 291 (hydrography+condition) and PLS1 of block 2 (Procrustes coordinates; correlation = 0.421, $P <$
 292 0.001). The maximum covariance related changes in salinity with displacements of the maxilla-
 293 dentary (LM3 and 4), mesethmoid (LM1) and opercle (LM20). This means that in brackish waters,
 294 eelpouts showed a slender head and snout, smaller eyes, and horizontally oriented mouth (Fig. 7, left

295 panel), while in saltier waters (more oceanic influenced areas), individuals had more robust head,
 296 shorter snout, bigger eyes and more oblique mouth opening (Fig. 7, right panel). The overall strength
 297 of association between blocks was low (Escoufier's RV = 0.058), but significant (permutation test, P
 298 < 0.001).

299



300

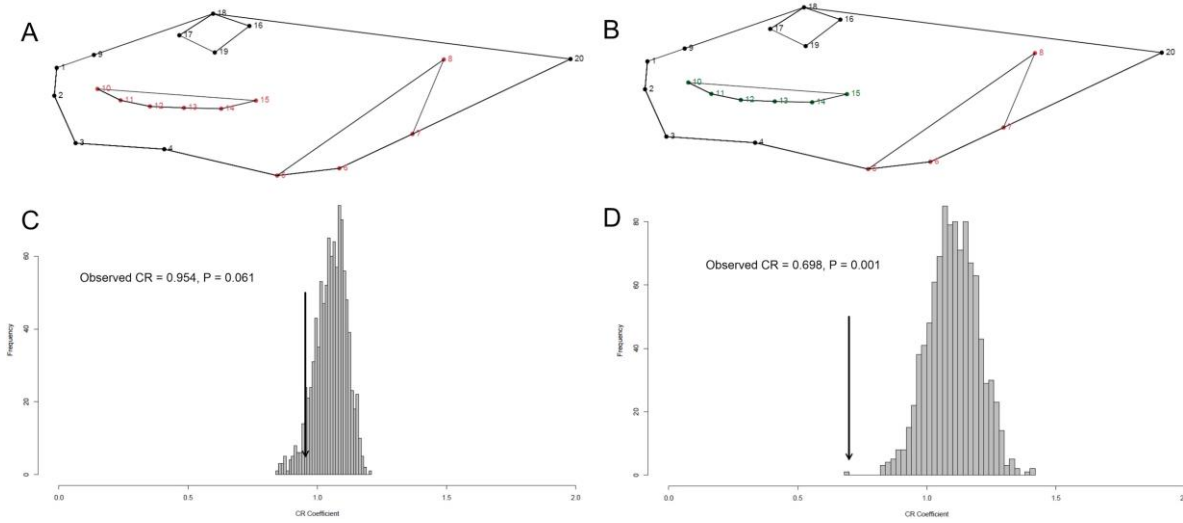
301 Figure 7. PLS showing covariance between condition indices (Fulton, Kn) and hydrographic
 302 conditions (sea temperature and salinity) (upper panel), and shape variability (lower panel). Grey
 303 wireframes represent the consensus shape, while the black wireframes represent the target shape
 304 related to fresher (left panel) and saltier waters (right panel).

305

306 Integration and modularity

307 Two hypotheses of modularity were tested. H1 (the *functional hypothesis*) compared the
 308 modularity between the shape of the head and the location of two peripheral lateral-line canals. Under
 309 this scenario, the observed CR was 0.954, showing that both head and canals are integrated in the
 310 development ($P = 0.061$, Fig. 8A, C). Nonetheless, As CR gets smaller ($CR < 1$), that means that
 311 within-module covariation is greater than between module covariation and that the structure is more

312 modular, H2 (the *structural hypothesis*) indicated that there is a significant modularity among three
313 modules: head, suborbital pores, and preoperculo-mandibular pores (CR = 0.698, $P = 0.001$, Fig. 8B,
314 D).



315

316 Figure 8. Hypothesis of integration and modularity between A, C) head (black dots) and sensory
317 canals (red dots), and B, D) head (black dots), suborbital pores (green dots) and preoperculo-
318 mandibular pores (red dots).

319

320 Discussion

321 In the eelpout *Austrolycus depressiceps* (4.5-22.5 cm TL), intraspecific phenotypic variability
322 of morphospace was detected in terms of individuals with larger, pointed snout and an extended
323 suborbital canal to individuals with shorter, rounded snout and frontally compressed suborbital canal.
324 These morphs represent ~40% of the shape variation, while the ontogenetic allometry was low (~5%),
325 represented by a decrease of the relative size of the eye, and a depression of the posterior margin of
326 the head. At scales of hundreds of kilometres, individuals inhabiting the northernmost locations
327 (45°S) showed robust heads while those from the southern tip of South America (55°S) showed a
328 slender head, with a pointed snout. Seawater salinity covaried with shape variability of the head; in
329 brackish waters, eelpouts showed a slender head and snout, smaller eyes, and horizontally oriented
330 mouth, while in saltier waters (more oceanic-influenced areas), individuals had more robust head,
331 shorter snout, bigger eyes and more oblique mouth opening. Additionally, two of the canals of the
332 cephalic lateralis pores and the head shape showed modularity in its development. This evidence

333 suggest ecomorphological interactions between the changing coastal environment and the eelpout
334 phenotype.

335 There are no previous studies using geometric morphometrics describing phenotypic
336 variability in the morphology of Zoarcidae. Nonetheless, recent studies using classic morphometrics,
337 suggests that Zoarcidae show high rates of shape evolution across several traits (Price et al. 2019). In
338 the family, phenotypic variation has been described in terms of vertebral counts of *Lycodapus*
339 *mandibularis* (Peden 1979), the positive allometry for body width and the complex of head characters
340 of *Lycodes yamatoi* (Savelyev et al. 2011), and the fluctuating asymmetry in the morphological
341 variation of *Zoarces viviparus* (Lajus et al. 2003). Our results indicate that the snout showed the
342 largest source of shape variation (large *vs.* short; pointed *vs.* rounded snout), as well as the relative
343 location of the two last pores of the suborbital canal. These morphological differences may cause
344 intraspecific variations in the feeding habits, like in some gobies (Vera-Duarte et al. 2017), and may
345 be linked to variations in salinity and turbidity along fjords and channels of west Patagonia (Castillo-
346 Hidalgo et al. 2018).

347 The ontogenetic allometry was low and mainly related to the change of the relative size of
348 the eye diameter. The eye size variability was previously described by Lloris and Rucabado (1992),
349 who detected that it might be contained between 9 and 16 times in the size of the head in specimens
350 between 9.8 and 41.1 cm TL. Generally, juveniles have larger eyes and heads relative to body size,
351 whereas, adults have smaller eyes and heads relative to body size (Ahlnelt et al. 2020). The change
352 in size of the head in relation to the eyes suggests the relevance of the sensory canals of the head as
353 the main source of information for predators and prey detection in adulthood.

354 Intraspecific variations in lateral-line anatomy and morphology, and their origin are not well
355 studied. Differences can be attributed to epigenetic effects (changes that affect gene activity and
356 expression without altering the DNA sequence) or to phenotypic plasticity (Mogdans 2019). In terms
357 of modularity, analyses showed a modular development between the suborbital and the preoperculo-
358 mandibular canals of the cephalic lateralis system. Pores of the cephalic system can be observed from
359 the hatching (Matallanas et al. 1990; Marcinkevicius & Gosztonyi 2013), but its relative location in
360 the head vary throughout early development, with larger displacements of the preoperculo-
361 mandibular canal than the suborbital canal in larval stages (Marcinkevicius & Gosztonyi 2013).
362 Additionally, intraspecific shape variability in juvenile and adults of *A. depressiceps* was focused on
363 the suborbital canal, while the preoperculo-mandibular canal showed slight variation only in PC2
364 (14% of the shape variation). Evidence, therefore, suggests an ontogenetic effect in the modularity of
365 head shape, suborbital and preoperculo-mandibular canals.

366 The West Patagonia shows important latitudinal gradients in the hydrographic features of the
367 coastal waters, such as temperature and salinity (Dávila et al. 2002; Saldías et al. 2019). The major
368 content of freshwater is located off central Patagonia, where the low-salinity surface layer dominates
369 the stratification of the upper ocean (Saldías et al. 2019). This latitudinal variability has significant
370 effects on several characteristics of marine fishes throughout the ontogeny, such as growth, survival
371 and bilateral symmetry (Landaeta et al. 2012, 2018; Molina-Valdivia et al. 2021). Additionally,
372 species with large latitudinal distribution show shallower bodies with a smaller head at higher
373 latitudes (Riesch et al. 2018), similar to our results. Other species that inhabit southern Patagonia,
374 such as the pike icefish *Champscephalus esox*, express similar phenotypic plasticity (Landaeta et al.
375 2021). Therefore, the hydrographic gradients may have imposed some constraints for the shape
376 variability of the head and sensory canals of *A. depressiceps*, i.e., phenotype modulation. In
377 phenotypic modulation, non-specific phenotypic variation results from the relative sensitivity of
378 various parts of the developing organism to primarily physical factors in the environment. Therefore,
379 this mechanism typically produces continuous phenotypic variation (Smith-Gill 1983), such as the
380 eelpout's morphs observed across Patagonia for a large salinity gradient (from 14 to 33).

381 A morphospace pattern related to water temperature has been observed in larval stages of
382 some blennioid species, showing taller bodies (head and trunk) when water temperature is warmer
383 (labrisomids genus *Auchenionchus* and *Calliclinus*, Landaeta et al. 2019, Galeano-Chavarría et al.
384 2020). Similarly, specimens collected in the southernmost locations (Beagle channel and Horn
385 Island), which show low seawater temperature (<4-9°C, Bruno et al. 2018), had hydrodynamic heads.
386 In the covariance analysis, temperature only had a secondary influence on the shape variability
387 (PLS2). However, temperature might be covarying also with salinity, particularly in central
388 Patagonia, where Icefields' retreat causes the intrusion of fresher, and colder waters (Landaeta et al.
389 2011, Bown et al. 2019).

390 Finally, future scenarios of climate change in the area will cause the freshening and cooling
391 of the coastal waters, because of the rapid retreat of Northern and Southern Patagonian icefields (Muto
392 & Furuya 2013, Bravo et al. 2021), and may cause important variations in the morphology of the
393 marine fish inhabiting Patagonia, particularly those utilizing shallow, coastal waters.

394

395 Acknowledgments

396 We thank the tourism company Cruceros Australis for logistical support during fieldwork in southern
397 Patagonia. Also, we thank Ernesto Davis and Pedro Contreras for their help with the fish collections.

398 Specimens were captured under the Chilean legislation (Technical Memorandum P.INV N° 224/2016
399 and N° E-2020-120 SUBPESCA).

400

401 **Literature cited**

402 Adams, D.C., 2016. Evaluating modularity in morphometric data: challenges with the RV coefficient
403 and a new test measure. *Methods in Ecology and Evolution* 7: 565-572. [https://doi.org/10.1111/2041-](https://doi.org/10.1111/2041-210X.12511)
404 [210X.12511](https://doi.org/10.1111/2041-210X.12511)

405 Adams, D.C., & E. Otárola-Castillo, 2013. geomorph: an r package for the collection and analysis of
406 geometric morphometric shape data. *Methods in Ecology and Evolution* 4: 393-399.
407 <https://doi.org/10.1111/2041-210X.12035>

408 Ahnelt, H., M. Sauberer, D. Ramler, L. Koch & C. Pogoreutz, 2020. Negative allometric growth
409 during ontogeny in the large pelagic filter-feeding basking shark. *Zoomorphology* 139: 71-83.
410 <https://doi.org/10.1007/s00435-019-00464-2>

411 Anderson, M.E., 1994. Systematics and osteology of the Zoarcidae (Teleostei: Perciformes).
412 *Ichthyological Bulletin of the JLB Smith Institute of Ichthyology* 60: 1-120.

413 Anderson, M.E. & V.V. Fedorov, 2004. Family Zoarcidae Swainson 1839 – eelpouts. *California*
414 *Academy of Science Annual Checklist Fish* 34: 1-58.

415 Anderson, M.E. & A.E. Gostonyi, 1991. Studies on the Zoarcidae (Teleostei: Perciformes) of the
416 Southern Hemisphere. IV. New records and a new species from the Magellan Province of South
417 America. *Ichthyological Bulletin of the JLB Smith Institute of Ichthyology* 55: 1-16.

418 Baken, E.K., M.L. Collyer, A. Kaliontzopoulou & D.C. Adams, 2021. geomorph v4.0 and gmShiny:
419 Enhanced analytics and a new graphical interface for a comprehensive morphometric experience.
420 *Methods in Ecology and Evolution*, 00, 1– 9. <https://doi.org/10.1111/2041-210X.13723>

421 Bookstein, F.L., 1992. *Morphometric Tools for Landmark Data*. Cambridge: Cambridge University
422 Press, 435 p.

423 Bown, F., A. Rivera, M. Petlicki, C. Bravo, J. Oberreuter & C. Moffat, 2019. Recent ice dynamics
424 and mass balance of Jorge Montt Glacier, Southern Patagonia Icefield. *Journal of Glaciology* 65: 732-
425 744. <https://doi.org/10.1017/jog.2019.47>

426 Bravo, C., D. Bozkurt, A.N. Ross & D.J. Quincey, 2021. Projected increases in surface melt and ice
427 loss for the Northern and Southern Patagonian Icefields. *Scientific Reports* 11: 16847.
428 <https://doi.org/10.1038/s41598-021-95725-w>

429 Bruno, D.O., M.F. Victorio, E.M. Acha & D.A. Fernández, 2018. Fish early life stages associated
430 with giant kelp forests in sub-Antarctic coastal waters (Beagle Channel, Argentina). *Polar Biology*
431 41: 365-375. <https://doi.org/10.1007/s00300-017-2196-y>

432 Castillo-Hidalgo, G., M.F. Landaeta, E. Anaya-Godínez & C.A. Bustos, 2018. Larval fish
433 assemblages from channels and fjords of south Pacific Patagonia: effects of environmental conditions.
434 *Revista de Biología Marina y Oceanografía* 53(S1): 39-49.
435 <https://doi.org/10.22370/rbmo.2018.53.0.1253>

436 Dávila, P.M., D. Figueroa & E. Müller, 2002. Freshwater input into the coastal ocean and its relation
437 with the salinity distribution off austral Chile (35–55° S). *Continental Shelf Research* 22: 521–534.
438 [https://doi.org/10.1016/S0278-4343\(01\)00072-3](https://doi.org/10.1016/S0278-4343(01)00072-3)

439 Fanta, E., F.S. Ríos, A.A. Meyer, S.R. Grötzner & T. Zaleski, 2001. Chemical and visual sensory
440 systems in feeding behaviour of the Antarctic fish *Ophthalmolycus amberensis* (Zoarcidae). *Antarctic*
441 *Record* 45: 27– 42.

442 Galeano-Chavarría, A.M., M.F. Landaeta, G. Plaza, M.I. Castillo & D.S. Alarcón, 2020.
443 Environmental determinants in morphospace and diet of the larval blenny *Calliclinus geniguttatus*
444 from an upwelling ecosystem. *Journal of Fish Biology* 97(6): 1808-1820.
445 <https://doi.org/10.1111/jfb.14544>

446 Goswami, A. & P.D. Polly, 2010. Methods for studying morphological integration and modularity.
447 In: *Quantitative Methods in Paleobiology*, J. Alroy & G. Hunt (eds.). The Paleontological Society
448 Papers, Vol. 6. 213-243 pp.

449 Gosztonyi, A.E., 1977. Results of the research cruises of FVR “Walther Herwig” to Southamerica.
450 XLIII. Revision of the Southamerican Zoarcidae (Osteichthyes, Blennioidei) with the description of
451 three new genera and five new species. *Archiv für Fischereiwissenschaft* 27: 191-249.

452 Hulton, N., Purves, P., McCulloch R., D. Sugden & M. Bentley, 2002. The Last Glacial Maximum
453 and deglaciation in southern South America. *Quaternary Science Reviews* 21: 233–241.
454 [https://doi.org/10.1016/S0277-3791\(01\)00103-2](https://doi.org/10.1016/S0277-3791(01)00103-2)

455 Hüne, M., 2019. Lista sistemática actualizada de los peces de Chile. Versión 1.4. Checklist dataset.
456 Global Biodiversity Information Facility. 2019. <https://doi.org/10.15468/er28jy>

457 Hüne, M., A.M. Friedlander, E. Ballesteros, J.E. Caselle & E. Sala, 2021. Assemblage structure and
458 spatial diversity patterns of kelp forest-associated fishes in Southern Patagonia. PLoS ONE 16:
459 e0257662. <https://doi.org/10.1371/journal.pone.0257662>

460 Klingenberg, C.P., 2011. MorphoJ: an integrated software package for geometric morphometrics.
461 Molecular Ecology Resources 11: 353-357. <https://doi.org/10.1111/j.1755-0998.2010.02924.x>

462 Klingenberg, C.P., 2013. Visualization in geometric morphometrics: how to read and how to make
463 graphs showing shape changes. Hystrix 24: 15-24. <https://doi.org/10.4404/hystrix-24.1-7691>

464 Lajus, D., R. Knust & O. Brix, 2003. Fluctuating asymmetry and other parameters of morphological
465 variation of eelpout *Zoarces viviparus* (Zoarcidae, Teleostei) from different parts of its distributional
466 range. Sarsia 88: 247-260. <https://doi.org/10.1080/00364820310001985>

467 Landaeta, M.F., C.A. Bustos, P. Palacios-Fuentes, P. Rojas & F. Balbontín, 2011. Distribución del
468 ictioplancton en la Patagonia austral de Chile: potenciales efectos del deshielo de Campos de Hielo
469 Sur. Latin American Journal of Aquatic Research 39: 236-249. [https://doi.org/10.3856/vol39-issue2-
470 fulltext-5](https://doi.org/10.3856/vol39-issue2-fulltext-5)

471 Landaeta, M.F., G. López, N. Suárez-Donoso, C.A. Bustos & F. Balbontín, 2012. Larval fish
472 distribution, growth and feeding in Patagonian fjords: potential effects of freshwater discharge.
473 Environmental Biology of Fishes 93: 73-87. <https://doi.org/10.1007/s10641-011-9891-2>

474 Landaeta, M.F., G. Castillo-Hidalgo & C.A. Bustos, 2018. Effects of salinity on larval growth and
475 otolith asymmetry of austral hake *Merluccius australis*. Latin American Journal of Aquatic Research
476 46: 212-218. <https://doi.org/10.3856/vol46-issue1-fulltext-20>

477 Landaeta, M.F., V. Bernal-Durán, M.I. Castillo, M. Díaz-Astudillo, B. Fernández-General & P.
478 Núñez-Acuña, 2019. Nearshore environmental conditions influence larval growth and shape changes
479 for a temperate rocky reef fish. Hydrobiologia 839: 159-176. [https://doi.org/10.1007/s10750-019-
480 04004-3](https://doi.org/10.1007/s10750-019-04004-3)

481 Landaeta, M.F., A. Villegas & M. Hüne, 2021. Shape, condition and diet of the pike icefish
482 *Champsocephalus esox* (Teleostei: Channichthyidae): evidence of phenotypic plasticity? Antarctic
483 Science 33(1): 10-16. <https://doi.org/10.1017/S0954102020000425>

484 Lannoo, M.J. & J.T. Eastman, 2006. Brain and sensory organ morphology in Antarctic eelpouts
485 (Perciformes, Zoarcidae, Lycodinae). Journal of Morphology 267: 115-127.
486 <https://doi.org/10.1002/jmor.10391>

487 Loris, D. & J. Rucabado, 1991. Ictiofauna del canal Beagle (Tierra del Fuego), Aspectos ecológicos
488 y análisis biogeográfico. Publicaciones Especiales Instituto Español de Oceanografía 8: 1-168.

489 Loy, A., L. Mariani, M. Bertelletti & L. Tunesi, 1998. Visualizing allometry: geometric
490 morphometrics in the study of shape changes in the early stages of the two-banded sea bream,
491 *Diplodus vulgaris* (Perciformes, Sparidae). Journal of Morphology 237: 137-146.

492 Marcinkevicius, M.S. & A.E. Gosztonyi, 2013. Early life history of three Patagonian zoarcids.
493 Revista de Biología Marina y Oceanografía 48: 285-292. [https://doi.org/10.4067/s0718-](https://doi.org/10.4067/s0718-19572013000200008)
494 [19572013000200008](https://doi.org/10.4067/s0718-19572013000200008)

495 Matallanas, J., 1988. Datos morfológicos y morfométricos del tracto alimentario de peces del canal
496 Beagle. Miscelanea Zoología 12: 235-243.

497 Matallanas, J., J. Rucabado, D. Lloris & M.P. Olivar, 1990. Early stages of development and
498 reproductive biology of the South-American eelpout *Austrolycus depressiceps* Regan, 1913
499 (Teleostei: Zoarcidae). Scientia Marina 54: 257-261.

500 Mogdans, J., 2019. Sensory ecology of the fish lateral-line system: Morphological and physiological
501 adaptations for the perception of hydrodynamic stimuli. Journal of Fish Biology 95: 53-72.
502 <https://doi.org/10.1111/jfb.13966>

503 Molina-Valdivia, V., C.A. Bustos, M.I. Castillo, F.V. Search, G. Plaza & M.F. Landaeta, 2021.
504 Oceanographic influences on the early life stages of a mesopelagic fish across the Chilean Patagonia.
505 Progress in Oceanography 195(3-4): 102572. <https://doi.org/10.1016/j.pocean.2021.102572>

506 Moreno, C.A. & H.F. Jara, 1984. Ecological studies on fish fauna associated with *Macrocystis*
507 *pyrifera* belts in the south of Fuegian Islands, Chile. Marine Ecology Progress Series 15: 99-107.

508 Muto, M. & M. Furuya, 2013. Surface velocities and ice-front positions of eight major glaciers in the
509 Southern Patagonian Ice Field, South America, from 2002 to 2011. Remote Sensing of the
510 Environment 139: 50-59. <https://doi.org/10.1016/j.rse.2013.07.034>

511 Ouyang, X., J. Gao, M. Xie, B. Liu, L. Zhou, B. Chen, J. Jourdan, R. Riesch & M. Plath, 2018. Natural
512 and sexual selection drive multivariate phenotypic divergence along climatic gradients in an invasive
513 fish. Scientific Reports 8: 11164. <https://doi.org/10.1038/s41598-018-29254-4>

514 Peden, A.E., 1979. Meristic variation of *Lycodapus mandibularis* (Pisces: Zoarcidae) and oceanic
515 upwelling on the West Coast of North America. Journal of the Fisheries Board of Canada 36: 69-76.
516 <https://doi.org/10.1139/f79-009>

517 Pequeño, G., 1986. Comments on fishes from the Diego Ramírez Island, Chile. Japanese Journal of
518 Ichthyology 32: 440-442. <https://doi.org/10.11369/jji1950.32.440>

519 Price, S.A., S.T. Friedman, K.A. Corn, C.M. Martinez, O. Larouche & P.C. Wainwright, 2019.
520 Building a body shape morphospace of Teleostean fishes. Integrative and Comparative Biology 59:
521 716-730. <https://doi.org/10.1093/icb/icz115>

522 Reyes, P. & M. Hüne, 2012. Peces del sur de Chile. Ocho Libros Editores, Santiago, 500 pp.

523 Riesch, R., R.A. Martin, S.E. Diamond, J. Jourdan, M. Plath & R.B. Langerhans, 2018. Thermal
524 regime drives a latitudinal gradient in morphology and life history in a livebearing fish. Biological
525 Journal of the Linnean Society 125: 126-141. <https://doi.org/10.1093/biolinnean/bly095>

526 Rohlf, F.J. & D.E. Slice, 1990. Extensions of the Procrustes method for the optimal superimposition
527 of landmarks. Systematic Zoology 39: 40-59.

528 Saldías, G.S., M. Sobarzo & R. Quiñones, 2019. Freshwater structure and its seasonal variability off
529 western Patagonia. Progress in Oceanography 174: 143-153.
530 <https://doi.org/10.1016/j.pocean.2018.10.014>

531 Savelyev, P.A., A.A. Balanov & V.A. Parensky, 2011. Allometric variation and sexual dimorphism
532 in *Lycodes yamato* Toyoshima, 1985 (Perciformes: Zoarcidae) from the Sea of Japan. Russian
533 Journal of Marine Biology 37: 33-41.

534 Smith-Gill, S.J., 1983. Developmental plasticity: Developmental conversion *versus* phenotypic
535 modulation. American Zoologist 23: 47-55.

536 Stearns, S.C., 1989. The evolutionary significance of phenotypic plasticity. BioScience 39: 436-445.

537 Sudgen, D.E., N. Hulton & R.S. Purves, 2002. Modelling the inception of the Patagonian icesheet.
538 Quaternary International 95–96: 55–64. [https://doi.org/10.1016/S1040-6182\(02\)00027-7](https://doi.org/10.1016/S1040-6182(02)00027-7)

539 Sultan, S.E., 2011. Evolutionary implications of individual plasticity. In: Transformations of
540 Lamarckism: From subtle fluids to molecular biology, S. B. Gissis & E. Jablonka (eds). MIT Press:
541 Cambridge, MA. 193-203 pp.

542 Valladares-Gómez, A., M. Huenumilla-Linares, E. Rodríguez-Serrano, C.E. Hernández & R.E.
543 Palma, 2020. Morphological variation in two sigmodontine rodents along the mainland and the
544 Fuegian archipelago in Chilean southern Patagonia. *Revista Chilena de Historia Natural* 93: 6.
545 <https://doi.org/10.1186/s40693-020-00094-9>

546 Vanella, F.A. & J. Calvo, 2005. Influence of temperature, habitat and body mass on routine metabolic
547 rates of Subantarctic teleosts. *Scientia Marina* 69: 317-323.
548 <https://doi.org/10.3989/scimar.2005.69s2317>

549 Vera-Duarte, J., C.A. Bustos & M.F. Landaeta, 2017. Diet and body shape changes of paroko
550 *Kelloggella disalvoi* (Gobiidae) from intertidal pools of Easter Island. *Journal of Fish Biology* 91:
551 1319-1336. <https://doi.org/10.1111/jfb.13450>

552 Voskoboinikova, O.S. & D.L. Laius, 2003. Osteological development of European eelpout *Zoarces*
553 *viviparus* (Zoaridae). *Journal of Ichthyology* 43: 646-659.

554